Research Article

Metabolic flux analysis of the two astaxanthin-producing microorganisms *Haematococcus pluvialis* and *Phaffia rhodozyma* in the pure and mixed cultures

Qing-Lin Dong, Xue-Ming Zhao, Hong-Wu Ma, Xiang-Ying Xing and Nai-Xia Sun

Department of Biochemical Engineering, School of Chemical Engineering and Technology, Tianjin University, Tianjin, PR China

The two major astaxanthin-producing microorganisms *Phaffia rhodozyma* and *Haematococcus pluvialis* exhibited elevated astaxanthin yields under the mixed culture regime, and the changes in flux distribution were investigated by means of metabolic flux analysis (MFA). In the mixed culture of the two strains, the carbon flux towards astaxanthin formation in *P. rhodozyma* increased by 20%, which may be due to the enriched oxygen evolved through the photosynthesis of *H. pluvialis*. On the other hand, the uptake of pyruvate and CO_2 excreted by *P. rhodozyma* also facilitated astaxanthin synthesis *in H. pluvialis,* which reduced 33% of the carbon flux exported from Calvin cycle to the catabolic pathway, and in turn raised the carbon flux to glyceraldehyde-3-phosphate by 25%. As a result, the carbon flux diverted to astaxanthin synthesis increased 2.8-fold in comparison with that in the pure culture.

Received 10 May 2006
Revised 1 September 2006
Accepted 21 September 2006

Keywords: Astaxanthin · *Haematococcus pluvialis* · Metabolic flux analysis · Mixed culture · *Phaffia rhodozyma*

1 Introduction

The high value-added ketocarotenoid astaxanthin is gaining increasing attention in recent years owing to its powerful antioxidant activity and potential applications in the pharmaceutical, nutritional, food and feed as well as aquaculture industries [1]. Among the astaxanthin-producing microorganisms found in nature, *Haematococcus pluvialis* and *Phaffia rhodozyma* are the two principal strains currently utilized for natural astaxanthin production [2, 3]. *H. pluvialis* is a unicellular green alga, which synthesizes and accumulates astaxanthin under stress conditions, such as nitrogen and phosphate limitations as well as salt stress and high light intensities [4–8]. *P. rhodozyma* is a red yeast, which produces astaxanthin growing on various organic substrates. Although extensive investigations have been carried out on both species aiming to improve the astaxanthin yields, the production levels, however, are still not high enough to commercially compete with the synthetic version [9]. In our previous works, increased biomass and astaxanthin yields were obtained by mix-cultivation of the two strains *H. pluvialis* and *P. rhodozyma* [10]. The underlying astaxanthin-synthesis-promoting mechanism was quite complicated and not well characterized. Therefore, a better understanding of the variations in astaxanthin-related metabolic activities within the two species under mixed culture regime is necessary and strongly desired.

During the last decade, a new trend in mathematical modeling has emerged by focusing on the so-called metabolic flux analysis (MFA), where intracellular fluxes are computed from the measured extracellular metabolites by using the stoichiometry of a metabolic network supposed to govern the system [11, 12]. Consequently, metabolic flux analysis has gained popularity as a technique to understand microbial processes, with the ultimate aim of improving productivity [13]. Nonetheless, despite the crucial importance of metabolic flux analysis as a helpful tool

Correspondence: Professor Xue-Ming Zhao, Department of Biochemical Engineering, School of Chemical Engineering and Technology, Tianjin University, Tianjin 300072, PR China
E-mail: xmzhao@tju.edu.cn
Fax: +86-22-2740-6770

Abbreviations: **EMP pathway**, Embden-Meyerhof-Pamas pathway; **GAP**, glyceraldehyde-3-phosphate; **IPP**, isopentenyl diphosphate; **PP pathway**, pentose phosphate pathway; **TCA**, tricarboxylic acid cycle

in designing metabolic engineering strategies, there is no reported work on the application of these tools for microbial isoprenoid production [14]. Thus, the aim of this study is to elucidate the changes in flux distribution by comparing the metabolic fluxes of *H. pluvialis* and *P. rhodozyma* in the pure and mixed cultures.

2 Materials and methods

2.1 Microorganisms and media

H. pluvialis and P. rhodozyma (AS2-1557) were obtained from Institute of Hydrobiology and Institute of Microbiology of Chinese Academy of Science, respectively. *H. pluvialis* was maintained at 4°C in a liquid BBM medium containing $NaNO_3$, 250 mg/L; $MgSO_4{\cdot}7H_2O$, 75 mg/L; NaCl, 25 mg/L; K_2HPO_4, 75 mg/L; KH_2PO_4, 175 mg/L; $CaCl_2{\cdot}2H_2O$, 25 mg/L; $ZnSO_4{\cdot}7H_2O$, 8.82 mg/L; $MnCl_2{\cdot}4H_2O$, 1.44 mg/L; MoO_3, 0.71 mg/L; $CuSO_4{\cdot}5H_2O$, 1.57 mg/L; $Co(NO_3)_2{\cdot}6H_2O$, 0.49 mg/L; $FeSO_4{\cdot}7H_2O$, 4.98 mg/L; H_3BO_3, 11.4 mg/L; KOH, 31 mg/L; and $EDTANa_2$, 50 mg/L. *P. rhodozyma* was maintained at 4°C on a slant of yeast malt agar (YM agar, Difco) containing (per liter) 10 g of glucose, 5.0 g of Bacto peptone, 3.0 g of malt extract, 3.0 g of yeast extract, and 20 g of agar. Pure culture of *H. pluvialis* was conducted on BBM while for mixed culture and pure culture of *P. rhodozyma*, a modified BBM medium (supplemented with 5 g/L glucose) was applied.

2.2 Cultivation conditions

The seed culture of *H. pluvialis* was prepared by transferring 5 mL of the alga liquid culture into a 500-mL flask containing 100 mL BBM medium. While, the seed culture of *P. rhodozyma* was prepared by inoculating the yeast from the fresh slant into a 500-mL flask containing 100 mL YM medium (glucose, 10 g/L; malt, 3 g/L; peptone, 5 g/L; yeast extract, 3 g/L). Both cultures were shaken at 110 rpm in an orbital shaker (with top cool white fluorescent lamps) at 23.8°C under the light intensity of 30 μmol photons/m^2 s for 48 h. Pre-cultures of *H. pluvialis* were conducted by transferring 10 mL seed cultures into 250-mL flasks containing 50 mL culture media. The flasks were incubated under 60 μmol photons/m^2 s constant light intensity at 23.8°C and 130 rpm in a rotary shaker for 120 h.

The batch cultures were conducted in a modified 5-L fermentor (BIOSTAT®B) containing 2 L media (initial pH 7.0), light was provided by eight cool white fluorescent lamps surrounded the fermentor with a incident intensity of 280 μmol photons/m^2 s. Airflow, agitation speed and temperature were maintain at 0.25 L/min, 150 rpm and 23.8°C, respectively. Inoculation of pure cultures of *H. pluvialis* and *P. rhodozyma* was carried out by transferring 200 mL and 50 mL pre-culture and seed cultures into the reactor, respectively, while for the mixed culture, both the *H. pluvialis* (200 mL) and the *P. rhodozyma* (50 mL) were inoculated.

2.3 Analyzing methods

Cells of *H. pluvialis* and *P. rhodozyma* in the samples of the mixed culture were separated by sucrose density gradient centrifugation as described in [15]. CO_2 and O_2 concentration in the off gas were determined using a gas analyzers (CO_2 analyzer, Telatre, USA and O_2 analyzer, Rae Systems, USA). Procedures for biomass estimation, astaxanthin quantification and residual sugar determination were conducted in the same way as detailed in our previous work [10].

For identification of the organic acid excreted by *P. rhodozyma* 5 mL sample from the flask was centrifuged at 5000 rpm for 10 min. The supernatant was used for identification of the acids by HPLC (Hewlett Packard series 1100, USA), using a Variable Wavelength Detector over an organic acids column (Eclipse×DB-C8, 4.6 × 150 mm). The mobile phase consisted of 0.005 M H_2SO_4, and the flow rate was kept at 0.6 mL/min. Peaks coming off the column were detected at 210 nm.

2.4 Metabolic network constructions and flux estimations

2.4.1 General comments

Genome-scale metabolic models for *P. rhodozyma* and *H. pluvialis* are unavailable because both strains have not been sequenced up to now. Alternatively, the metabolic networks of the two strains were constructed based on the relevant investigations on yeast, green algae and/or higher plants.

2.4.2 Metabolic network of P. rhodozyma

In the present study, the organic acids excreted by *P. rhodozyma* were identified as pyruvate by HPLC analysis. The primary metabolic network including Embden-Meyerhof-Pamas pathway (EMP pathway), pentose phosphate pathway (PP pathway) and TCA cycle (tricarboxylic acid cycle) was constructed based on the previous investigation [16] (Fig. 1; the subsequent bioreactions are summarized in Appendix A). As to the astaxanthin-related secondary metabolism, it has been demonstrated that yeast and fungi only take the acetate/mevalonate (MAV) pathway, using acetyl-CoA as the original precursor to form the common "brick" of isopentenyl diphosphate (IPP) and astaxanthin [17, 18]. Furthermore, several steps involved in the reaction from acetate to astaxanthin are not well-characterized up to date [19]. Therefore, in the present study, the whole linear sequence of reactions from acetyl-CoA to astaxanthin are briefly considered as two steps for simplicity and easy calculation, which are the formation of IPP from acetyl-CoA and in turn the reaction from IPP to astaxanthin, provided that no other IPP-derived compounds were formed.

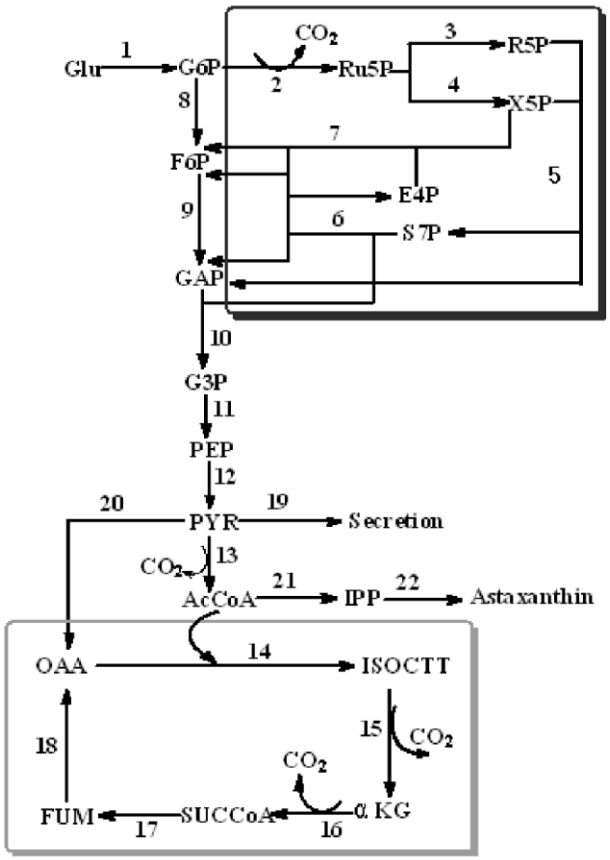

Figure 1. The metabolic network of *P. rhodozyma* in the pure and mixed cultures. Abbreviations: **AcCoA**, acetyl-coenzyme A; **α-KG**, α-ketoglutarate; **E4P**, erythrose-4-phosphate; **F6P**, fructose-6-phosphate; **FUM**, fumarate; **G3P**, 3-phosphoglycerate; **G6P**, glucose-6-phosphate; **GAP**, glyceraldehyde-3-phosphate; **Glu**, glucose; **IPP**, isopentenyl diphosphate; **ISOCIT**, isocitrate; **OAA**, oxaloacetate; **PEP**, phosphoenolpyruvate; **PYR**, pyruvate; **R5P**, ribose-5-phosphate; **Ru5P**, ribulose-5-phosphate; **S7P**, sedoheptulose-7-phosphate; **SUCCoA**, succinyl-coenzyme A; **X5**P, xylulose-5-phosphate.

Table 1. Biomass and astaxanthin content of *H. pluvialis* growing in pure, mixed and pyruvate–added cultures[a)]

Cultures	Pure culture	Mixed culture	Pyruvate-added culture
Initial biomass (g/L)	0.31	0.31	0.31
Final biomass (g/L)	0.52	0.92	0.86
Initial astaxanthin (mg/g)	0.00	0.00	0.00
Final astaxanthin (mg/g)	1.12	2.88	2.59
Initial pyruvate (g/L)	0.00	0.00	0.60
Final pyruvate (g/L)	0.00	0.03	0.02

a) The cultivation period is 5 days.

2.4.3 *Metabolic networks of H. pluvialis*

To find out if pyruvate produced by *P. rhodozyma* could be assimilated by *H. pluvialis*, we cultivated *H. pluvialis* in pure, mixed (adding glucose 3.0 g/L) and pyruvate-added (adding 0.6 g/L pyruvate) cultures, respectively. The experiment was conducted in the same way as described in the pre-culture (Section 2.2), except that (i) the light intensity was adjusted to 160 μmol photons/m^2 s, and (ii) the mixed culture was inoculated with both *H. pluvialis* and *P. rhodozyma*. The results are shown in Table 1. It can be seen that biomass and astaxanthin yields obtained in mixed culture were the highest, followed by those of pyruvate-added and pure cultures. These results strongly suggest that pyruvate generated by *P. rhodozyma* could be assimilated by *H. pluvialis* for both cell growth and astaxanthin formation.

The primary metabolic network of *H. pluvialis* was built according to the relevant investigations on algae and higher plants [20–25], where, the parallel EMP and PP pathways operating in the chloroplast and cytoplasm were integrated (Fig. 2). The reactions within the network are listed in Appendix B. Additionally it should be noted that *H. pluvialis* possess only quite limited capability to utilize glucose compared with the red yeast [10]. Thus, the only organic substrate assimilated by *H. pluvialis* in the mixed culture was pyruvate excreted by *P. rhodozyma*. The assimilated pyruvate was divided into two parts: one part was used preferably for IPP synthesis, as it is the original precursor of IPP while the other was directed to acetyl-CoA along EMP pathway and then entered TCA cycle to generate reducing power and produce amino acids for mass build-up.

With respect to the secondary metabolism, astaxanthin formation in *H. pluvialis* differs from *P. rhodozyma* in that it takes MEP (2-*C*-methyl-D-erythritol 4-phosphate) pathway for the synthesis of IPP, via incorporation of the two initiating compounds glyceraldehyde 3-phosphate (GAP) and pyruvate [26]. Moreover, just like the case in *P. rhodozyma*, the biosyntheses of astaxanthin from GAP and pyruvate are briefly considered as a two-step reaction.

2.4.4 *Metabolic flux estimations*

For the metabolic flux analysis of *H. pluvialis*, the biomass compositions including protein, carbohydrates, crude fat as well as amino acids and fatty acids were obtained from The Technical Report of *Haematococcus pluvialis* algal meal (Mera Pharmaceuticals 1999. AstaFactor® Technical Report: Typical composition of Nutraxan™ Asta dried *Haematococcus pluvialis* algal meal), while DNA and RNA contents were taken the same as *Chlorella pyrenoidosa* [27]. As for *P. rhodozyma*, the detailed biomass compositions reported by Johnson's research group [28] were applied.

It was assumed that *P. rhodozyma* produced same amounts of pyruvate and CO_2 under pure and mixed culture regimes. Subsequently, the specific evolution rates of pyruvate and CO_2 of *P. rhodozyma* growing in the mixed

Biotechnol. J. 2006, 1, 1283–1292

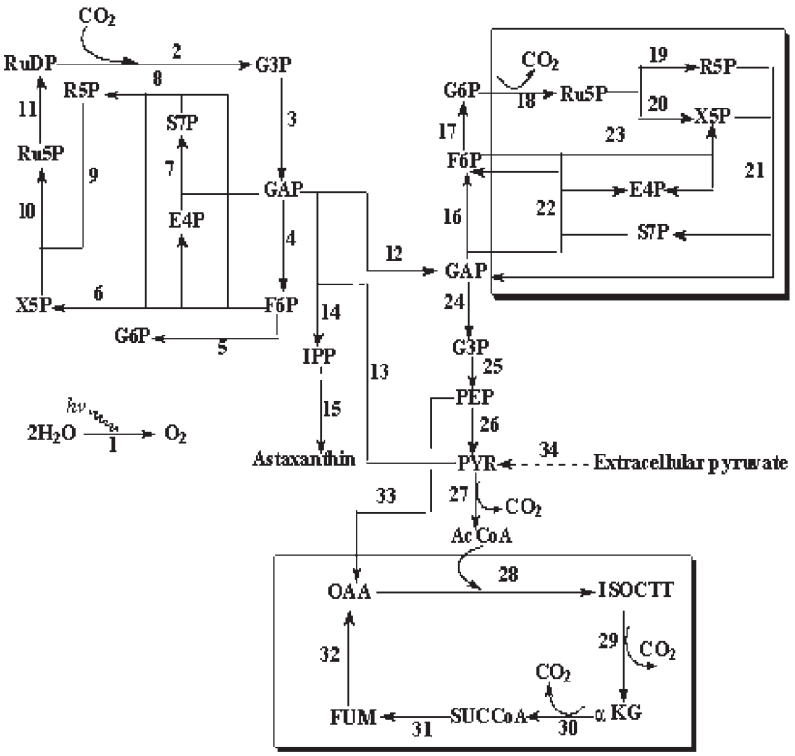

Figure 2. The metabolic network of *H. pluvialis* in the pure and mixed cultures. Dashed line indicates the uptake of extracellular pyruvate by *H. pluvialis* in the mixed culture.

culture were calculated according to their productions in the pure culture. The reduced pyruvate and CO_2 in the mixed culture compared to the pure culture of *P. rhodozyma* were considered being assimilated by *H. pluvialis*, as both cultures were conducted under the same conditions.

Prior to flux analysis, the data were analyzed for the presence of measurement errors using elemental balances [29]. It was shown that the elemental balances for C (input/output 1.03) and N (input/output 1.01) could be closed. Flux calculations were carried out according to the mass balancing method using the software of MATLAB. A series of stoichiometric equations (Appendix A and B) combined with the metabolite measurements were applied to estimate the intracellular fluxes based on the equation $S \times \nu = 0$, where S is a stoichiometric matrix and ν is the specific reaction rate.

3 Results and discussion

3.1 Cultivation of *P. rhodozyma* and *H. pluvialis* under different culture regimes

Pure and mixed cultures of *P. rhodozyma* and *H. pluvialis* were all carried out in a batch mode as detailed in the Section 2.2. The time profiles of biomass and astaxanthin as well as the glucose, pyruvate, CO_2 evolution and uptake rates in the pure and mixed culture are presented in Figs. 3–9, and the experimental results are summarized in Table 2.

As shown in Figs. 3–6, astaxanthin yields of *H. pluvialis* and *P. rhodozyma* in the mixed culture were both higher than those in the pure cultures were. Furthermore, the biosynthesis of astaxanthin in *H. pluvialis* proceeded continually after the cell growth ceased, indicating that astaxanthin formation is non-growth-associated, at least during the later phase. By contrast, astaxanthin synthesis in *P. rhodozyma* appeared to be dependent on cell growth.

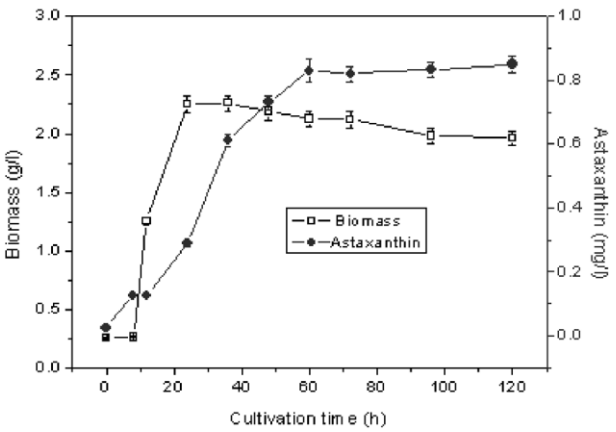

Figure 3. Time course of the biomass and astaxanthin of *P. rhodozyma* in the pure culture. All the results presented are the mean value of three replicates. Vertical bars represent SD ($n = 3$).

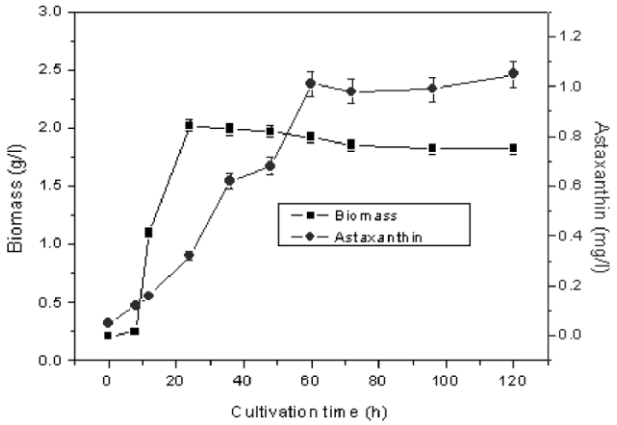

Figure 4. Time course of the biomass and astaxanthin of *P. rhodozyma* in the mixed culture. All the results presented are the mean value of three replicates. Vertical bars represent SD ($n = 3$).

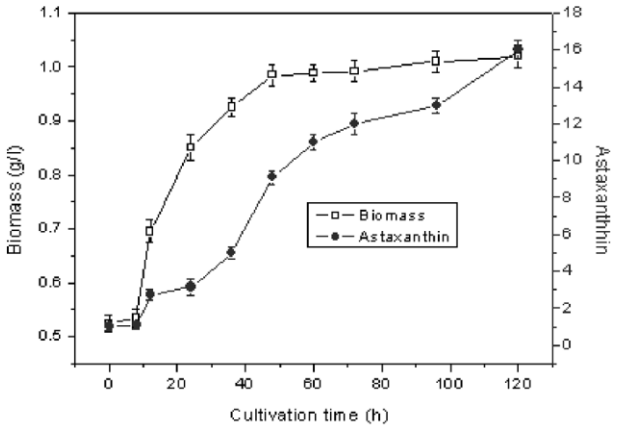

Figure 5. Time course of the biomass and astaxanthin in the pure culture of *H. pluvialis*. All the results presented are the mean value of three replicates. Vertical bars represent SD ($n = 3$).

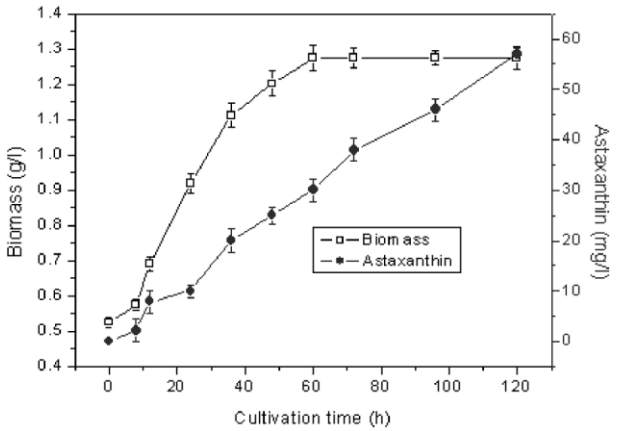

Figure 6. Time course of the biomass and astaxanthin of *H. pluvialis* in the mixed culture. All the results presented are the mean value of three replicates. Vertical bars represent SD ($n = 3$).

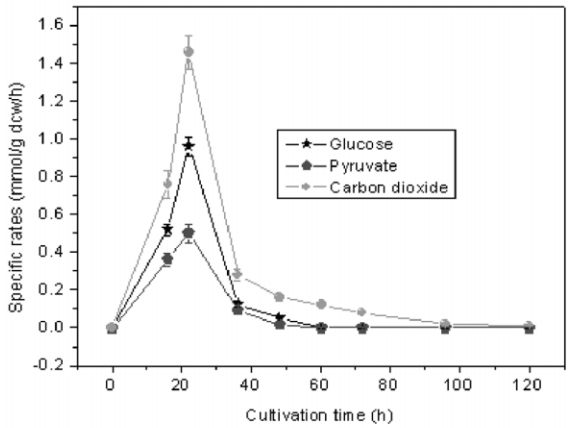

Figure 7. The specific glucose uptake as well as pyruvate and CO_2 production rates in the pure culture of *P. rhodozyma*. All the results presented are the mean value of three replicates. Vertical bars represent SD ($n = 3$)

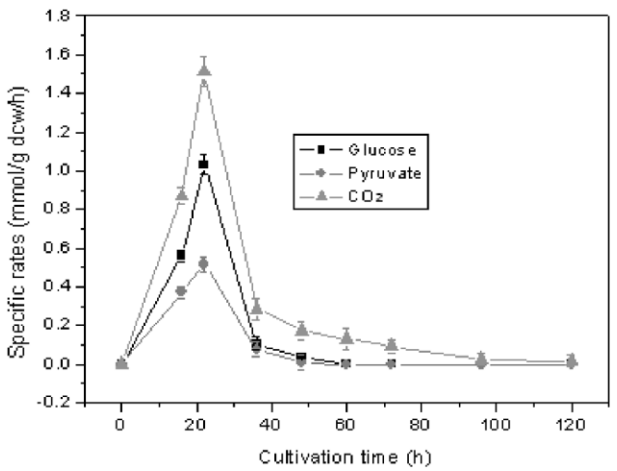

Figure 8. The specific glucose uptake as well as pyruvate and CO_2 production rates in the mixed culture. All the results presented are the mean value of three replicates. Vertical bars represent SD ($n = 3$)

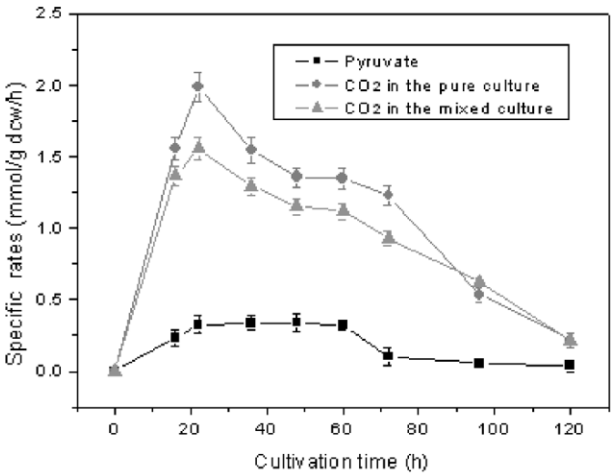

Figure 9. The specific pyruvate and CO_2 uptake rates in the pure and mixed cultures. All the results presented are the mean value of three replicates. Vertical bars represent SD ($n = 3$)

Table 2. The test results of *P. rhodozyma* and *H. pluvialis* in the pure and mixed cultures[a)]

Parameters	*H. pluvialis*		*P. rhodozyma*	
	Pure culture	Mixed culture	Pure culture	Mixed culture
Specific growth rate μ	0.026	0.039	0.068	0.066
Specific CO_2 uptake rate mmol/g (dcw[b)])/h	1.56	1.99	----	----
Specific pyruvate uptake rate mmol/g (dcw)/h	----	0.326	----	----
Specific astaxanthin formation rate mmol/g (dcw)/h	0.0092	0.026	$2.62–10^{-5}$	$3.11–10^{-5}$
Specific glucose consumption rate mmol/g (dcw)/h	----	----	0.962	1.08
Specific CO_2 evolution rate mmol/g (dcw)/h	----	----	1.46	1.51
Specific pyruvate formation rate mmol/g (dcw)/h	----	----	0.501	0.516
Specific O_2 uptake rate mmol/g (dcw)/h	-----	-----	1.52	1.68
Biomass (g/L)	0.96	1.32	2.26	2.05
Ysx (g/g)	----	----	0.45	0.402

a) The uptake of CO_2, O_2 and pyruvate by *H. pluvialis* was calculated by comparison of their concentrations in the pure culture of *P. rhodozyma* and the mixed culture. The specific rates represent the values at 22 h.

b) Dry cell weight.

3.2 Metabolic flux analysis of *P. rhodozyma*

As shown in Fig. 10, the carbon flux towards astaxanthin synthesis increased by 20% in the mixed culture compared to that of the pure culture. This may be due to the elevated oxygen consumption rate (Table 2), because astaxanthin formation requires oxygen and higher oxygen consumption stimulates astaxanthin synthesis [30, 31].

Pyruvate is a key branch-point between EMP pathway and TCA cycle located at the major junction of assimilatory and dissimilatory reactions. As shown in Fig. 10, most of the carbon influx from glucose catabolism (69% in the pure culture and 72% in the mixed culture) converged on the pyruvate node. However 37% (pure culture) and 35% (mixed culture) of these fluxes drained off the EMP pathway and then excreted into the medium. These results suggest that the relatively higher flux towards pyruvate node and lower percent of pyruvate secretion in the mixed culture were responsible for the elevated astaxanthin production, as it modulates the flux to acetyl-CoA (the originating precursor for astaxanthin formation) downstream.

The split ratios between PP and EMP pathways at the G-6-P node were around 1:1, in both pure and mixed cultures, with 48 and 51% of the carbon influx being directed to PP pathway, respectively. These results are lower than in the previous report [16], which showed that about 66% of the glucose was consumed via the PP pathway. One reason for this may be the different strain and different culture conditions used in the experiments. The other is that the former calculation did not take the pyruvate secretion into account, where CO_2 was considered as the sole excreted product.

The relatively high PP flux exhibited in the mixed culture may be indicative of the increasing energy requirement for astaxanthin synthesis, because astaxanthin formation in the microorganisms is a highly energy-dependent bioprocess [32], and the PP pathway is commonly known to supply reducing power for the biosynthetic processes at the expense of carbon loss in the form of CO_2.

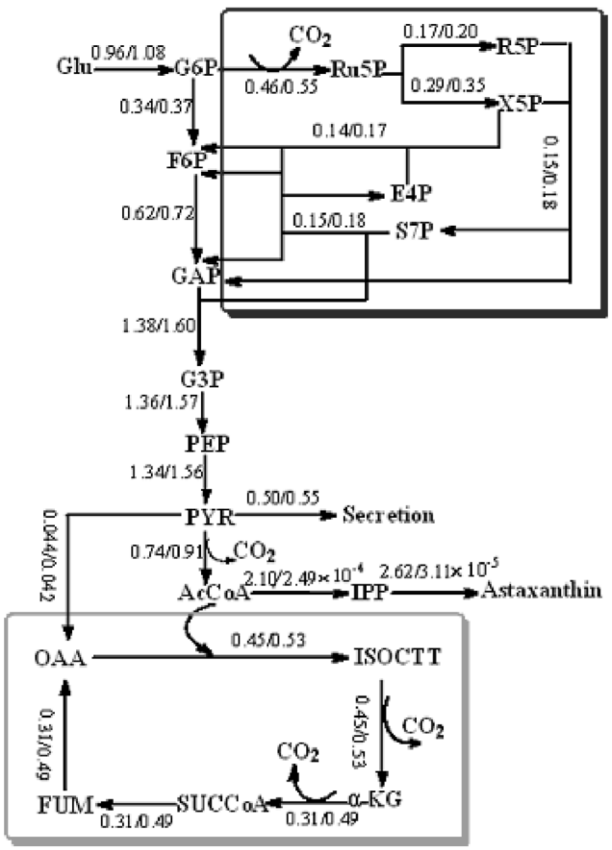

Figure 10. The flux distributions of *P. rhodozyma* in the pure and mixed cultures. Specific fluxes are expressed as mmol/g dry cell weight (DCW) per hour, representing the flux distribution at 22 h. The left and right-hand numerals are the fluxes in the pure and mixed cultures, respectively.

This relationship could explain, at least in part, why lower biomass but higher astaxanthin were obtained in the mixed culture. It appears likely that in *P. rhodozyma*, the enzymes surrounding glucose-6-phosphate (G6P) node are sufficiently flexible to permit optimal allocation of carbon fluxes between glycolysis and the PP cycle to generate more reducing power for astaxanthin synthesis in response to environmental perturbations.

Additionally, considering the high flux of pyruvate leakage, we are led to conclusion that a remarkable malic enzyme activity may be performed in *P. rhodozyma* for maintaining the cytosolic pyruvate level, similarly as in the case of oleaginous yeast, *e.g. Saccharomyces cerevisiae*.

3.3 Metabolic flux analysis of *H. pluvialis*

3.3.1 Flux distribution

As shown in Fig. 11, the flux distribution among different pathways within the entire metabolic network varied significantly in *H. pluvialis* under both pure and mixed culture regimes. The carbon flux in Calvin cycle was much higher than that in the catabolic network. Furthermore, in the catabolic network, most of the carbon flux flowed along the EMP pathway with only minor flux being directed to the PP pathway and TCA cycle. These results indicate that (i) Calvin cycle played a principal role in controlling the entire flux distribution and, (ii) the EMP pathway was the major route for carbon catabolism, while PP pathway and TCA cycle in *H. pluvialis* were likely to operate in flexible manner for intermediate supply.

3.3.2 Carbon flux towards astaxanthin

Carbon flux towards astaxanthin synthesis in the mixed culture increased up to threefold compared to that in the pure culture. The reason for this is, of course, the increased supply of the two originating compounds, pyruvate and GAP, as the key factor for high-yield of astaxanthin production in microorganisms is the sufficient supply of precursors [33].

3.3.3 Pyruvate node

In the pure culture of *H. pluvialis*, pyruvate was a glycolytic intermediate and originated indirectly from the

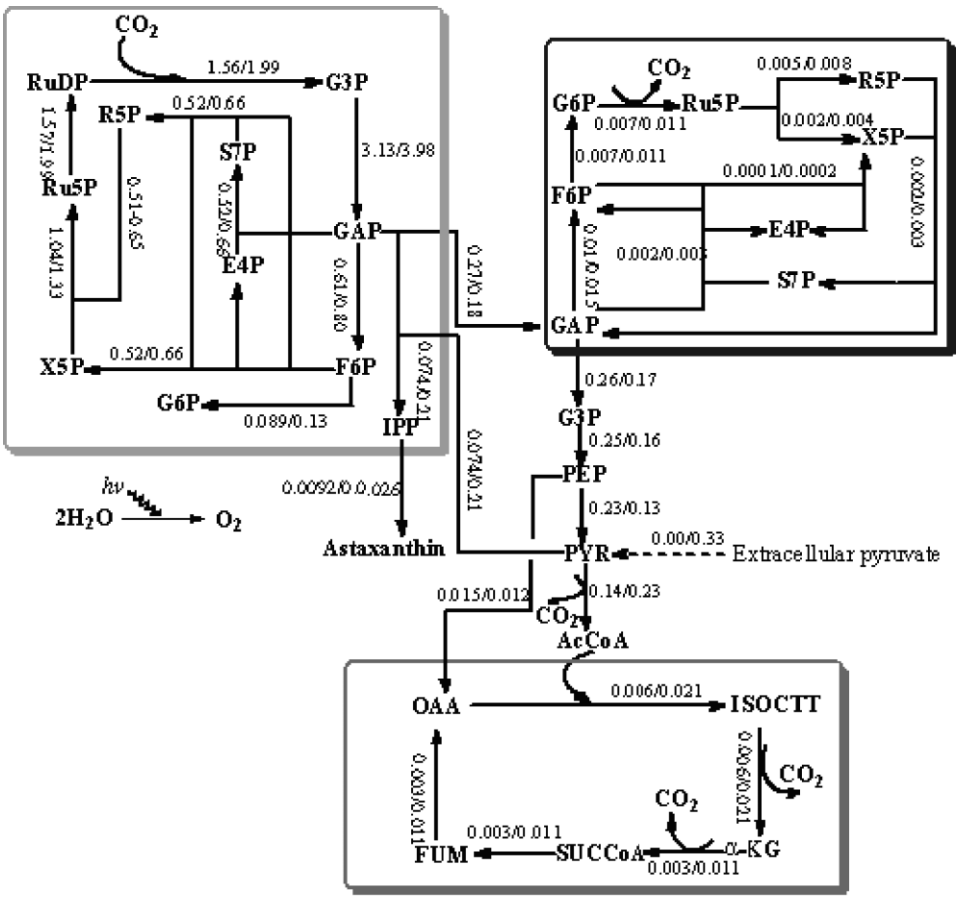

Figure 11. The specific flux distributions of *H. pluvialis* in the pure and mixed cultures. The fluxes are expressed as mmol/g DCW per hour, representing the flux distribution at 22 h. The left and right-hand numerals are the fluxes in the pure and mixed cultures, respectively.

GAP exported from the Calvin cycle. Thus, the carbon flux towards pyruvate was dependent, absolutely, on the amount of GAP imported, and only 85% of the imported flux was funneled into the pyruvate node. Since both pyruvate and GAP are utilized in equal amounts in the formation of astaxanthin, apparently, pyruvate in the pure culture was not in equilibrium with GAP and became the limiting factor governing astaxanthin synthesis. By contrast, the small supply of pyruvate was overcome in the mixed culture, where the carbon flux to pyruvate increased by twofold due to the uptake of extracellular pyruvate produced by *P. rhodozyma*.

3.3.4 GAP node in Calvin cycle

The flux towards GAP node located at the Calvin cycle in the mixed culture increased 25% in comparison with that of the pure culture. The reason for this comes from two aspects. First, the uptake of pyruvate in the mixed culture reduced the carbon flux channeled from Calvin cycle for maintaining the operation of PP pathway and TCA cycle. Consequently, GAP exported from Calvin cycle into the catabolic network declined by 33%. Secondly, increased influx at the Ru5P node in the Calvin cycle via enhanced incorporation of ambient CO_2 promoted the level of 3-phosphoglycerate. Subsequently, carbon flux towards GAP increased by 27% compared to that of the pure culture.

From the results discussed above, it is reasonable to conclude that GAP node located at Calvin cycle and pyruvate node in EMP pathway are the key branch points, because they control the carbon flux towards astaxanthin synthesis.

4 Concluding remarks

The results of the metabolic flux analysis in the present study show that the carbon flux towards astaxanthin formation in *P. rhodozyma* increased 20% under the mixed culture regime, which may be due to the enriched oxygen evolved by *H. pluvialis* and the increased oxygen consumption rate. In *H. pluvialis*, the main carbon flux was directed along Calvin cycle. GAP and pyruvate nodes located at Calvin cycle and EMP pathways, respectively, play crucial roles in controlling carbon flux to astaxanthin formation. The carbon flux towards astaxanthin synthesis increased 2.8-fold due to the increased supply of the originating precursor and the optimal balance between GAP and pyruvate.

Financial support was provided by the National Natural Science Foundation of China (NSFC-20536040) and the National Project of Key Fundamental Research (2003CB716003).

5 References

[1] Guerin, M., Huntley, M. E., Olaizola, M., *Haematococcus astaxanthin*: applications for human health and nutrition. *Trends Biotechnol.* 2003, *21*, 210–216.

[2] Margalith, P. Z., Production of ketocarotenoids by microalgae. *Appl. Microbiol. Biotechnol.* 1999, *51*, 431–438.

[3] Johnson, E. A., Schroeder, W. A., Microbial carotenoids. *Adv. Biochem. Eng. Biotechnol.* 1995, *53*, 119–178.

[4] Boussiba, S., Carotenogenesis in the green alga *Haematococcus pluvialis*: Cellular physiology and stress response. *Physiol. Plant* 2000, *108*, 111–117.

[5] Borowitzka, M. A., Huisman, J. M., Osborn, A., Culture of the astaxanthin-producing green alga *Haematococcus pluvialis*. 1. Effects of nutrients on growth and cell type. *J. Appl. Phycol.* 1991, *3*, 295–304.

[6] Fábregas, J., Dománguez, A., Garcíýa-Álvarez, D., Lamela, T., Otero, A., Induction of astaxanthin accumulation by nitrogen and magnesium deficiencies in *Haematococcus pluvialis*. *Biotechnol. Lett.* 1998, *20*, 623–626.

[7] Harker, M., Tsavalos, A. J., Young, A. J., Factors responsible for astaxanthin formation in the chlorophyte *Haematococcus pluvialis*. *Bioresource Technol.* 1996, *55*, 207–214.

[8] Kobayashi, M., Kakizono, T., Nagai, S., Enhanced carotenoid biosynthesis by oxidative stress in acetate-induced cyst cells of a green unicellular alga, *Haematococcus pluvialis*. *Appl. Environ. Microbiol.* 1993, *59*, 867–873.

[9] Olaizola, M., Commercial development of microalgal biotechnology: From the test tube to the marketplace. *Biomol. Eng.* 2003, *20*, 459–466.

[10] Dong, Q. L., Zhao, X. M., *In situ* carbon dioxide fixation in the process of natural astaxanthin production by a mixed culture of *Haematococcus pluvialis* and *Phaffia rhodozyma*. *Catal. Today* 2004, *98*, 537–544.

[11] Stephanopoulos, G. N., Aristidou, A. A.,Nielsen, J., (Ed.) *Metabolic Engineering*, Academic press, San Diego 1998.

[12] Provost, A., Bastin, G., Dynamic metabolic modelling under the balanced growth condition. *J. Process Contr.* 2004, *14*, 717–728.

[13] Gombert, A. K., Santos, M. M., Christensen, B., Nielsen, J., Network identification and flux quantification in the central metabolism of *Saccharomyces cerevisiae* under different conditions of glucose repression. *J. Bacteriol.* 2001, *183*, 1441–1451.

[14] Maury, J., Asadollahi, M. A., Møller, K., Clark, A., Nielsen, J., Microbial isoprenoid production: An example of green chemistry through metabolic engineering. *Adv. Biochem. Engin/Biotechnol.* 2005, *100*, 19–51.

[15] Masuda, K., Kudo-Shiratort, A., Inane, M., Callus formation and plant regeneration from rice protoplasts purified by density gradient centrifugation. *Plant Sci.* 1989, *62*, 237–246.

[16] Cannizzaro, C., Christensen, B., Nielsen, J., von Stockar, U., Metabolic network analysis on *Phaffia rhodozyma* yeast using ^{13}C–labeled glucose and gas chromatography-mass spectrometry. *Metab. Eng.* 2004, *6*, 340–351.

[17] Schwender, J., Seemann, M., Lichtenthaler, H. K., Romer, M., Biosynthesis of isoprenoids (carotenoids, sterols, prenyl side-chains of chlorophylls and plastoquinone) via a novel pyruvate/glyceraldehydes 3-phosphate non-mevalonate pathway in the green alga *Scenedesmus obliquus*. *Biochem. J.* 1996, *316*, 73–80.

[18] Spurgeon, S. L., Porter, J. W., (Ed.) *Biosynthesis of Isoprenoid Compounds*, John Wiley and Sons, New York 1981.

[19] Sanpietro, L. M. D., Kula, M. R., Studies of astaxanthin biosynthesis in *Xanthophyllomyces dendrorhous* (*Phaffia rhodozyma*). Effect of inhibitors and low temperature. *Yeast* 1998, *14*, 1007–1016.

[20] Rontein, D., Dieuaide-Noubhani, M., Dufourc, E. J., Raymond, P., Rolin, D., The metabolic architecture of plant cells: Stability of cen-

tral metabolism and flexibility of anabolic pathways during the growth cycle of tomato cells. *J. Biol. Chem*. 2002, *277*, 43948–43960.
[21] Schwender J., Ohlrogge J. B, Shachar-Hill Y., A flux model of glycolysis and the oxidative pentosephosphate pathway in developing *Brassica napus* embryos. *J. Biol. Chem.* 2003, *278*, 29442–29453.
[22] Morgan, J. A., Rhodes, D., Mathematical modeling of plant metabolic pathways. *Metab. Eng*. 2002, *4*, 80–89.
[23] Armbrust, E. V. Berges, J. A., Bowler, C., Green, B. R. *et al.*, The Genome of the diatom *Thalassiosira Pseudonana*: ecology, evolution, and metabolism. *Science* 2004, *306*, 79–86.
[24] Schwender, J., Ohlrogge J., Shachar-Hill Y., Understanding flux in plant metabolic networks. *Curr. Opin. Plant Biol.* 2004, *7*, 309–317.
[25] Yang, C., Hua, Q., Shimizu, K., Metabolic flux analysis in *Synechocystis* using isotope distribution from ^{13}C-labeled glucose. *Metab. Eng*. 2002, *4*, 202–216.
[26] Rohmer, M., Knani, M., Simonin, P., Sutter, B., Sahm, H., Isoprenoid biosynthesis in bacteria: a novel pathway for the early steps leading to isopentyl diphosphate. *Biochem J*. 1993, *295*, 517–524.
[27] Wanka, F., Joosten, H. F. P., Grip, W. J. de, Composition and synthesis of DNA in synchronously growing cells of *Chlorella pyrenoidosa*. *Arch. Mikrobiol.* 1970, *75*, 25–36.
[28] Johnson, E. A., Villa, T. G., Lewis, M. J., *Phaffia rhodozyma* as an astaxanthin source in salmonid diets. *Aquaculture* 1980, *20*, 123–134.
[29] Wang, N. S., Stephanopoulos, G., Application of macroscopic balances to the identification of gross measurement errors, *Biotechnol. Bioeng*. 1983, *25*, 2177–2208.
[30] Johnson, E. A., Lewis, M. J., Astaxanthin formation by the yeast *Phaffia rhodozyma*. *J. Gen. Microbiol*. 1979, *115*, 173–183.
[31] Yamane, Y. I., Higashida, K., Nakashimada, Y., Kakizono, T., Nishio, N., Influence of oxygen and glucose on primary metabolism and astaxanthin production by *Phaffia rhodozyma* in batch and fed-batch cultures: Kinetic and stoichiometric analysis. *Appl. Environm. Microbiology* 1997, *63*, 4471–4478.
[32] Misawa, N., Shimada, H., Metabolic engineering for the production of carotenoids in non-carotenogenic bacteria and yeasts. *J. Biotechnol*. 1998, *59*, 169–181.
[33] Wang, C. W., Oh, M. K., Liao, J. C., Engineered isoprenoid pathway enhances astaxanthin production in *Escherichia coli*. *Biotechnol. Bioeng*. 1999, *62*, 235–241.

Appendix A. Biochemical reactions in *P. rhodozyma*

Abbreviations: **AcCoA**, acetyl-coenzyme A; **α-KG**, α-ketoglutarate; **E4P**, erythrose-4-phosphate; **F6P**, fructose-6-phosphate; **FUM**, fumarate; **G3P**, 3-phosphoglycerate; **G6P**, glucose-6-phosphate; **GAP**, glyceraldehyde-3-phosphate; **Glu**, glucose; **IPP**, isopentenyl diphosphate; **ISOCIT**, isocitrate; **OAA**, oxaloacetate; **PEP**, phosphoenolpyruvate; **PYR**, pyruvate; **R5P**, ribose-5-phosphate; **Ru5P**, ribulose-5-phosphate; **S7P**, sedoheptulose-7-phosphate; **SUCCoA**, succinyl-coenzyme A; **X5**P, xylulose-5-phosphate

Glucose uptake

1. Glucose (extracellular) +ATP → G6P (cytoplasm) +ADP

PP-pathway (cytoplasm)

2. G6P+ 2NADP+ H_2O → Ru5P + CO_2+2NADPH+2H
3. Ru5P → R5P
4. Ru5P → X5P
5. R5P + X5P → S7P + GAP
6. S7P + GAP → F6P + E4P
7. X5P + E4P → G6P + GAP

EMP-pathway (cytoplasm)

8. G6P → F6P
9. F6P+ ATP → 2GAP+ADP+H
10. GAP+ NAD+ ADP+ Pi → G3P+NADH+ATP+H
11. G3P → PEP+H_2O
12. PEP+ ADP → PYR+ATP

TCA-cycle (mitochondrion)

13. PYR+CoA+NAD → AcCoA + CO_2+NADH+H
14. OAA + AcCoA+H_2O → ISOCIT + CoA + H
15. ISOCIT+ NAD → αKG+CO_2+NADH
16. αKG + CoA+ NAD → SUCCoA+ CO_2+NADH +H
17. SUCCoA+FAD+ADP+Pi → FUM+CoA+$FADH_2$+ATP
18. FUM+NAD+H_2O → OAA+NADH+H

Secretion of pyruvate

19. PYR (cytoplasm) → PYR (extracellular)

Anaplerotic reaction (cytoplasm)

20. PYR + CO_2 → OAA

Astaxanthin formation(cytoplasm)

21 3 AcCoA → IPP+C
22 8 IPP+NADH+$FADH_2$ → Astaxanthin+ NAD+FAD

23. **Intracellular metabolites used for biosynthesis of macromolecules (biomass)**

Biomass 0.510 G6P + 0.376 F6P + 0.399 R5P + 0.421E4P + 0.238 GAP + 1.53 PEP+3.62 PYR +3.96 ACA + 1.13 OAA+0.886 α-KG

Biotechnol. J. 2006, 1, 1283–1292

Appendix B. Biochemical reactions in *H. pluvialis*

Light reaction (chloroplast)

1. $2H_2O+2NADP+2ADP+2Pi+0.125APF \rightarrow O_2+2NADPH+2H+2.6ATP$

Calvin cycle (chloroplast)

2. $RuDP+CO_2+H_2O \rightarrow 2G3P$
3. $G3P+ATP+NADPH+H \rightarrow GAP+ADP+NADP+Pi$
4. $2GAP+H_2O \rightarrow F6P+Pi$
5. $F6P \rightarrow G6P$
6. $G6P+GAP \rightarrow X5P+E4P$
7. $E4P+GAP+H_2O \rightarrow S7P+Pi$
8. $S7P+GAP \rightarrow R5P+X5P$
9. $R5P \rightarrow Ru5P$
10. $X5P \rightarrow Ru5P$
11. $Ru5P+ATP \rightarrow RuDP+ADP+Pi$

Transport of GAP from chloroplast to cytoplasm

12. $GAP \rightarrow GAP$

Transport of pyruvate from cytoplasm to chloroplast

13. $PYR \rightarrow PYR$

Drain of GAP for astaxanthin synthesis (chloroplast)

$GAP \rightarrow GAP$

Astaxanthin formation (chloroplast)

14. $GAP+PYR \rightarrow IPP+C$
15. $8\,IPP+NADH+FADH_2 \rightarrow Astaxanthin+NAD+FAD$

EMP and PP pathways (cytoplasm and chloroplast)

16. $2GAP+H_2O \rightarrow F6P+Pi$
17. F6PG6P
18. $G6P+H_2O+2NADP \rightarrow Ru5P+CO_2+2NADPH+2H$
19. $Ru5P \rightarrow R5P$
20. $Ru5P \rightarrow X5P$
21. $R5P+X5P \rightarrow S7P+GAP$
22. $S7P+GAP \rightarrow F6P+E4P$
23. $F6P+GAP \rightarrow X5P+E4P$
24. $GAP+NAD+ADP+Pi \rightarrow G3P+NADH+H+ATP$
25. $G3P \rightarrow PEP+H_2O$
26. $PEP+ADP \rightarrow PYR+ATP$

TCA cycle (mitochondrion)

27. $PYR+NAD+CoA \rightarrow AcCoA+CO_2+NADH+H$
28. $OAA+AcCoA+H_2O \rightarrow ISOCIT+CoA+H$
29. $ISOCIT+NAD \rightarrow \alpha\text{-KG}+CO_2+NADH$
30. $\alpha\text{-KG}+CoA+NAD \rightarrow SUCCoA+NADH+CO_2+H$
31. $SUCCoA+ADP+Pi+FAD \rightarrow FUM+CoA+FADH_2+ATP$
32. $FUM+H_2O+NAD \rightarrow OAA+NADH+H$

Anaplerotic reaction (cytoplasm)

33. $PEP+CO_2+ADP \rightarrow OAA+ATP$

Uptake of extracellular pyruvate (only occurred in the mixed culture)

34. PYR (extracellular) → PYR (cytoplasm)

35. **Intracellular metabolites used for biosynthesis of macromolecules (biomass)**

Biomass 0.460 G6P + 0.362 F6P + 0.399 R5P + 0.406 E4P + 0.238 GAP + 1.53 PEP + 2.64 PYR +4.64 ACA + 1.23 OAA+1.04 α-KG